THE FLOW OF A RAREFIED GAS THROUGH A CIRCULAR ORIFICE AND A TWO-DIMENSIONAL SLIT

Thesis by

Nathan Raymond Thach, Jr.

In Partial Fulfillment of the Requirements

For the Degree of

Aeronautical Engineer

California Institute of Technology

Pasadena, California

1969

(Submitted September 23, 1968)

ACKNOWLEDGMENTS

I am deeply grateful to the Fannie and John Hertz Foundation for the generous financial support given me during my graduate study at the California Institute of Technology.

Sincere thanks go to F. T. Linton for his help with equipment modification; to my wife for her understanding and for typing the thesis; and to my friends for their encouragement.

ABSTRACT

Experiments were conducted to measure the mass flow of helium through a circular orifice and a two-dimensional slit over a wide range of Reynolds number for large pressure ratios across the test apertures. The Reynolds number, defined as $Re = \frac{D}{\nu_1}\sqrt{\frac{p_1 - p_2}{\rho_1}}$ for the orifice and $Re = \frac{2b}{\nu_1}\sqrt{\frac{p_1 - p_2}{\rho_1}}$ for the slit, ranged nominally from 5×10^{-2} to 3×10^{2}. The upstream-to-downstream pressure ratio, $p_1 : p_2$, was at all times greater than 100:1 so that the Mach number, defined as $Ma = \sqrt{1 - \frac{p_2}{p_1}}$, was at all times approximately unity.

The results of the present experiments on the circular orifice are found to compare favorably with the results of experimental and theoretical work on the circular orifice by previous investigators. The results of the present experiments on the two-dimensional slit (which appear to be the first of this nature) do not compare favorably with the results of the meager amount of theoretical work on the two-dimensional slit.

The transition from free-molecule flow to continuum-limit flow for the circular orifice appears to be substantially complete within the range $10^{-2} \leq \frac{Ma}{Re} \leq 10^{0}$. The two-dimensional slit behaves very much like the circular orifice for $\frac{Ma}{Re} \geq 10^{0}$. Unlike the circular orifice, however, the transition from free-molecule flow to continuum-limit flow for the two-dimensional slit appears to cover the range $\sim 10^{-4} \leq \frac{Ma}{Re} \leq 10^{0}$.

TABLE OF CONTENTS

LIST OF FIGURES

LIST OF SYMBOLS

atm	atmosphere
B	constant
b	short side of slit
C	centigrade
$\bar{c}$	mean molecular speed
cc	cubic centimeter
cm	centimeter
D	diameter of circular orifice
dA	elemental area
dV	elemental volume
exp	exponentiation
F	Fahrenheit
H_2O	water
Hg	mercury
hr	hour
h	long side of slit
Kn	Knudsen number
L	length of aperture in the flow direction
Ma	Mach number
m	mass
$\dot{m}$	mass flow rate
mm	millimeter
N	number density of molecules

LIST OF SYMBOLS (continued)

n	number of molecules
$\dot{n}$	number flow rate (of molecules)
p	pressure
$\overline{p}$	$\frac{1}{2}(p_1 + p_2)$
Δp	$p_1 - p_2$
psi	pounds force per square inch
psia	pounds force per square inch absolute
psig	pounds force per square inch gage
Q	collision cross section
R	gas constant per unit mass
Re	Reynolds number
r	distance from dV to dA
sec	second
T	absolute temperature
V	volume
W	characteristic velocity
X	power (magnification)
%	per cent
α	ratio of thin aperture mass flow to smooth nozzle mass flow
γ	ratio of specific heats
ϵ	mean number of collisions of a molecule per unit length traveled
θ	angle formed by r and the normal to dA

LIST OF SYMBOLS (continued)

κ	Clausing factor
λ	mean free path
μ	dynamic viscosity
ν	kinematic viscosity
ρ	density
μ	microns of mercury pressure

Subscripts

CL	continuum limit
fm	free-molecule limit
1	equilibrium state upstream of the aperture
2	equilibrium state downstream of the aperture
c	critical
i	state 1 or 2
j	state 1 or 2
$\frac{L}{D}$	length-to-diameter ratio

Superscripts

o	degree
.	rate
*	characteristic
"	inches
®	trademark

I. INTRODUCTION

Historically, the study of gas flow has been fragmented according to certain phenomena associated with the degree of gas rarefaction. For example, the study of gas flow with rarefaction parameter very much greater than unity (Knudsen number $Kn >> 1$) has been treated by the gaskinetic theory of molecular flow; and the study of gas flow with rarefaction parameter very much less than unity (Knudsen number $Kn << 1$) has been treated by the gasdynamic theory of continuum flow. Recently, however, much work has been expended in an effort to develop a unified gas flow analysis which is valid for any degree of rarefaction.

The basis for such a unified analysis is expected to be the description of gas flow by the method of statistical mechanics. At the present time, free-molecule flow is quite adequately described by the gaskinetic theory; nearly free-molecule flow can be analyzed by iteratively solving the gaskinetic equation; continuum flow can be described by macroscopic equations derived from the gaskinetic equation which are similar to the classical Navier-Stokes equations; and slip flow can be analyzed by the Navier-Stokes equations plus boundary condition modifications based on gaskinetic theory. Therefore, the transition flow between slip flow and nearly free-molecule flow should be amenable to analysis by some ad hoc equations which have their basis in gaskinetic theory.

Liepmann (1)[1] was the first to point out the experimental simplicity and well-posed theoretical beauty of the problem of flow through a thin aperture (i.e., a sharp-edged aperture with $L/D^* < 1$) and its usefulness in the development of a unified analysis of gas flow. He performed the first experiments directed toward the formulation of a basis for a complete rarefied gas flow analysis, and these experiments verified the soundness of his experimental approach and initial theoretical analysis. Since the publication of the paper describing his work and analysis, many other investigators have sought to make a contribution to this area of knowledge. In particular, the works of Willis (2), Sreekanth (3), Narasimha (4), Milligan (5), Smetana (6), Carley (7), and Lord (8) are worthy of note.

Following Liepmann's example, the problem of flow through a thin aperture is studied with the objective of contributing to a better understanding of the transition from free-molecule to continuum flow and the development of a unified analysis of gas flow.

---

[1]Numbers in parentheses refer to similarly numbered references in the Bibliography.

II. THEORY

Consider the steady flow of a gas from one large container to another through a thin aperture of arbitrary geometry. The subscript 1 denotes the location of an equilibrium state upstream of the aperture, and the subscript 2 denotes the location of an equilibrium state downstream of the aperture. Depending upon the degree of rarefaction of the gas, the flow can range from molecular effusion to potential flow.

Limit of Free-Molecule Flow

This end of the flow spectrum is characterized by a gas density so low, or an aperture so small, that the ratio of the mean free path of a gas molecule to the characteristic dimension of the aperture is much greater than unity (Knudsen number $Kn >> 1$). Under these conditions, a molecule will ordinarily pass from one container to the other without making any collisions in the neighborhood of the aperture. No mass motion of the gas develops, and the lack of reflected molecules from the area of the aperture has a negligible effect on the equilibrium-distribution function of the gas in each container. Therefore, the number of molecules n passing through an aperture of area A in each direction per unit time can be obtained from the elementary, gaskinetic theory calculation of the number of molecules n which strike an area A of the wall per unit

time. From Present (9), this number is

$$\dot{n} = \tfrac{1}{4}(NA\bar{c}) = \tfrac{1}{4}NA\sqrt{\frac{8RT}{\pi}} \quad , \tag{2-1}$$

where N is the number density of molecules at state 1 or 2, $\bar{c}$ is the mean molecular speed, R is the gas constant per unit mass, and T is the absolute temperature at state 1 or 2. The mass flow corresponding to equation (2-1) is

$$\dot{m} = \rho A\sqrt{\frac{RT}{2\pi}} \quad , \tag{2-2}$$

where ρ is the gas density at state 1 or 2.

For apertures of nonzero thickness, equation (2-2) must be multiplied by the Clausing (10) transmission probability factor for the particular aperture geometry. Thus, one obtains

$$_1\dot{m}_2 = {}_1\kappa_2 A_1 \rho_1\sqrt{\frac{RT_1}{2\pi}} \tag{2-3a}$$

and

$$_2\dot{m}_1 = {}_2\kappa_1 A_2 \rho_2\sqrt{\frac{RT_2}{2\pi}} \quad , \tag{2-3b}$$

where $_i\dot{m}_j$ is the mass flow in the direction from state i to state j and $_i\kappa_j$ is the Clausing factor for flow in the corresponding direction.

Since the flow is thermodynamically the Joule-Thomson process for the perfect gas, the temperature at state 2 is identical to that at state 1. The net flow through the aperture is then given by

$$\dot{m}_{fm} = ({}_1\kappa_2 \rho_1 A_1 - {}_2\kappa_1 \rho_2 A_2) \sqrt{\frac{RT_1}{2\pi}} \quad . \tag{2-4}$$

If the aperture geometry is symmetric with respect to a reversal of the flow, then ${}_2\kappa_1 A_2 = {}_1\kappa_2 A_1$. The net flow through the aperture is then

$$\dot{m}_{fm} = \kappa A(\rho_1 - \rho_2) \sqrt{\frac{RT_1}{2\pi}} \quad . \tag{2-5}$$

Using the ideal gas equation of state,

$$p = \rho RT \quad , \tag{2-6}$$

where p is the gas pressure, one may write

$$\dot{m}_{fm} = \frac{\kappa A(p_1 - p_2)}{\sqrt{2\pi RT_1}} \quad . \tag{2-7}$$

For the circular orifice, $1 \leq \kappa \leq \frac{4D}{3L}$. For the two-dimensional slit, $1 \leq \kappa \leq \frac{b}{L} \ln \frac{L}{b}$.

Near the Limit of Free-Molecule Flow

Nearly free-molecule flow is very much like free-molecule flow; however, the ratio of mean free path to characteristic aperture dimension is large and finite (Knudsen number Kn > 1), and the lack of reflected molecules from the area of the aperture does have an effect on the distribution function of the gas in each container. This part of the flow spectrum is best analyzed by iteratively solving the gaskinetic equation to obtain the non-equilibrium distribution function which can be integrated to give the number of molecules passing through the aperture per unit time and, consequently, the mass flow. This method has been applied to the circular orifice by Narasimha (4) and Willis (2) and to the two-dimensional slit by Willis (2). The computations are very long and laborious, and they usually require a number of simplifying assumptions. Narasimha found the leading terms of the first iterate to be

$$\left.\frac{\dot{m}}{\dot{m}_{fm}}\right|_{\text{orifice}} = 1 + 0.078\left(\frac{Ma}{Re}\right)^{-1} \quad . \qquad (2\text{-}8)$$

Willis found the leading terms of the first iterate to be

$$\left.\frac{\dot{m}}{\dot{m}_{fm}}\right|_{\text{orifice}} = 1 + 0.083\left(\frac{Ma}{Re}\right)^{-1} \qquad (2\text{-}9)$$

and

$$\left.\frac{\dot{m}}{\dot{m}_{fm}}\right|_{slit} = 1 - 0.0285\left(\frac{Ma}{Re}\right)^{-1}\ln\left(\frac{Ma}{Re}\right)^{-1} + 0.03725\left(\frac{Ma}{Re}\right)^{-1} \quad . \quad (2\text{-}10)$$

A less rigorous analysis of this part of the flow spectrum is found in Liepmann (1). He computes the number of molecules, scattered from a volume element dV in the direction of an element of area dA, which do not suffer a collision between dV and dA. Noting that the primary effect of the aperture is the reduction of the number of molecules in the neighborhood of the opening due to the lack of reflections, he obtains

$$\frac{\dot{m}}{\dot{m}_{fm}} = 1 + \frac{\frac{1}{8}}{\frac{\lambda}{D}} \pm \cdots \quad . \quad (2\text{-}11)$$

For the sake of comparison, a mean free path is defined by $\mu = \frac{1}{2}\bar{c}\rho\lambda$ so that one may write Liepmann's result as

$$\left.\frac{\dot{m}}{\dot{m}_{fm}}\right|_{orifice} = 1 + 0.0997\left(\frac{Ma}{Re}\right)^{-1} \quad . \quad (2\text{-}12)$$

One notes that the approach to the limit is quite slow. Equations (2-8) through (2-12) are based on the assumption of no molecular backflow. Although equations (2-8) and (2-9) differ by only a few

per cent, Willis has pointed out that Narasimha's result is rather fortuitous since his simplifying assumptions yield compensating errors.

Limit of Continuum Flow

This end of the flow spectrum is characterized by a gas density so high or an aperture so large that the ratio of the mean free path of a gas molecule to the characteristic dimension of the aperture is much less than unity (Knudsen number $Kn << 1$). Under these conditions, a molecule sustains many collisions in the neighborhood of the aperture; and a mass motion of the gas develops. Generally, because of the large number of collisions in the gas, the gas exhibits the properties of a continuum, and the gaskinetic analysis is abandoned in favor of the more familiar Navier-Stokes equations of gasdynamics. Strictly speaking, however, the gaskinetic analysis is still used; for the Navier-Stokes equations can be derived from the gaskinetic equation.

Consider the flow through the given aperture for infinite Reynolds number and large upstream-to-downstream pressure ratio p_1/p_2. (These conditions are equivalent to Knudsen number $Kn << 1$.) For inviscid flow, there exists a definite critical pressure ratio $(p_1/p_2)_c$ beyond which the downstream conditions cannot influence the upstream conditions. The maximum mass flow through the aperture, for given upstream conditions, is reached for this value of $(p_1/p_2)_c$. For a smooth nozzle, the critical pressure ratio and maximum mass flow can

be found from the one-dimensional, channel flow equations. They are

$$\left[\frac{p_1}{p_2}\right]_c = \left[\frac{\gamma+1}{2}\right]^{\frac{\gamma}{\gamma-1}} \tag{2-13}$$

and

$$\dot{m} = \rho_1 A \left[\gamma RT_1 \left(\frac{2}{\gamma+1}\right)^{\frac{\gamma+1}{\gamma-1}}\right]^{\frac{1}{2}} , \tag{2-14}$$

where γ is the ratio of specific heats of the gas. Unlike the free-molecule flow limit, one notes that the mass flow at the continuum limit is a function of the molecular complexity of the gas.

Whereas the sonic line (surface) in a smooth nozzle is approximately straight (planar), that in a sharp-edged aperture is double s-shaped (warped). Thus, in the plane of the aperture, the flow is mixed; it is partially subsonic and partially supersonic. Since the largest mass flow density occurs at local sonic velocity, the mass flow through an aperture is less than that through a smooth nozzle of comparable throat area. Hence, one writes for the aperture,

$$\dot{m}_{CL} = \alpha \rho_1 A \left[\gamma RT_1 \left(\frac{2}{\gamma+1}\right)^{\frac{\gamma+1}{\gamma-1}}\right]^{\frac{1}{2}} , \tag{2-15}$$

where $\alpha = \alpha(\gamma) \leq 1$.

The flow through a two-dimensional slit has been analyzed by Guderley (11) by the method of characteristics. The critical pressure ratio is found to be that necessary for a 45° turn from sonic in Prandtl-Meyer flow.

The computation of the corresponding mass flow is much more difficult. Only one calculation seems ever to have been made. Frankl (12) computed (numerically) the flow through a two-dimensional slit for $\gamma = 1.40$. His result was $\alpha = 0.85$.

The flow through a circular orifice is very difficult to analyze. Unlike the two-dimensional slit, the characteristics of the equation for the circular orifice in the hodograph plane are not known independently of the flow in the physical plane. Liepmann (1) gives an argument to show that the critical pressure ratio for the circular orifice should be greater than that for a slit and that the mass flow should be somewhat less. He argues that the difference should be very slight.

Near the Limit of Continuum Flow

For flow near the continuum limit, the ratio of mean free path to characteristic aperture dimension is small and finite (Knudsen number $Kn < 1$), and viscous effects must be considered in the analysis of the flow. A search of the available literature does not reveal any complete analysis of this part of the flow spectrum for the geometry under consideration. Liepmann (1) gives some qualitative and quantitative arguments which point toward a mass flow formula of the type

$$\frac{\dot{m}}{\dot{m}_{CL}} = 1 - \frac{1}{2\sqrt{Re}} \pm \cdots \quad . \tag{2-16}$$

When expressed in the variables used in the present study, this equation is

$$\frac{\dot{m}}{\dot{m}_{CL}} = 1 - \frac{1}{2}\left(\frac{Ma}{Re}\right)^{\frac{1}{2}} \pm \cdots \quad . \tag{2-17}$$

Slip and Transition Flow

Slip flow is that part of the flow spectrum where the Navier-Stokes equations still apply, but the no-slip boundary condition of conventional gasdynamics is relaxed to allow a velocity tangent to the bounding surface. Transition flow is that part of the flow spectrum between the slip flow and the nearly free-molecule flow which is identified by a mean free path to characteristic aperture dimension ratio of order unity (Knudsen number $Kn \sim 1$).

There do not appear to be any analyses for slip flow through thin apertures (if indeed there can be slip flow through thin apertures); however, Sreekanth (3) has initiated the unjustified practice (which has spread to other investigators) of fitting his transition flow data with the modified Poiseuille equation. This practice is discussed here strictly as a matter of record.

Following Present (9), one can obtain the mass flow formula

for slip flow in long circular tubes as

$$\dot{m} = \frac{\pi D^4 \bar{P} \Delta P}{128 \mu_1 R T_1 L} + B \frac{D^3 \Delta P}{\bar{c}_1 L} \quad , \tag{2-18}$$

where D is the tube diameter, L is the tube length, $\bar{p} = \frac{1}{2}(p_1 + p_2)$, $\Delta p = p_1 - p_2$, and B is a constant which is a function of the equation chosen to relate mean free path and viscosity.

For example, three common equations used to relate mean free path and viscosity are

$$\mu = \frac{1}{3} \bar{c} \rho \lambda \quad , \tag{2-19a}$$

$$\mu = \frac{5\pi}{32} \bar{c} \rho \lambda \quad , \tag{2-19b}$$

and

$$\mu = \frac{1}{2} \bar{c} \rho \lambda \quad . \tag{2-19c}$$

The B's associated with these relationships are respectively

$$B = \frac{\pi}{8} \quad , \tag{2-20a}$$

$$B = \frac{\pi}{4} - \frac{4}{15} \quad , \tag{2-20b}$$

and

$$B = \frac{\pi}{6} \quad . \tag{2-20c}$$

From equation (2-7), the free-molecule mass flow rate through a long tube is

$$\dot{m}_{fm} = \kappa A \frac{\Delta p}{\sqrt{2\pi RT}} \quad , \tag{2-21}$$

where $\kappa \Big|_{\frac{L}{D}\to\infty} = \frac{4D}{3L}$ and $A = \frac{\pi D^2}{4}$.

Dividing equation (2-18) by equation (2-21), one obtains

$$\frac{\dot{m}}{\dot{m}_{fm}} = \frac{3}{2}B + \frac{3\sqrt{2\pi}}{256} \frac{1 + \frac{p_2}{p_1}}{\frac{\mu_1\sqrt{RT_1}}{p_1 D}} \quad . \tag{2-22}$$

Note that for the pressure ratios considered here, p_2/p_1 is approximately zero, and equation (2-22) can be written as

$$\frac{\dot{m}}{\dot{m}_{fm}} \doteq \frac{3}{2}B + \frac{3\sqrt{2\pi}}{256}\left(\frac{Ma}{Re}\right)^{-1} \quad . \tag{2-23}$$

Unfortunately, equation (2-22) is invalid, for it is linear in $\bar{p}$; whereas, the experiments of Knudsen (13) and others have established the existence of a relative minimum in the mass flow ratio for flow in long tubes at low pressures such that the Knudsen number is of order unity. Moreover, the viscous flow theory with slip correction is

invalid for Knudsen number of order unity and, consequently, should not be extrapolated into this region.

Sreekanth (3) found that he could fit his experimental data for transition flow through circular orifices and short tubes ($L/D \leq 1$) with the right-hand side of equation (2-18) times the factor $L/(L + D)$. In his work, he does not indicate what led him to this choice, nor does he seem to grasp the significance of this parameter. Its relation to the present analysis in equations (2-18) through (2-23) is best seen when written as

$$\frac{L}{L+D} = \frac{\frac{L}{D}}{1+\frac{L}{D}} = \frac{1}{\frac{1+\frac{L}{D}}{\frac{D}{L}}} = \frac{4}{3}\frac{1}{\frac{1+\frac{L}{D}}{\frac{4D}{3L}}} = \frac{4}{3}\frac{\kappa\left|\frac{L}{D}\leq 1\right.}{\kappa\left|\frac{L}{D}\longrightarrow\infty\right.} \quad . \qquad (2\text{-}24)$$

When written in this form, one can easily note the effect of multiplying the right-hand side of equation (2-18) by $L/(L + D)$ which is to approximate the Clausing factor for long tubes by D/L and the Clausing factor for short tubes by $1/(1 + L/D)$. The D/L representation is quite poor (always 25% or more too small) since the Clausing factor for circular geometries has the range $1 \rightarrow 4D/3L$. The $1/(1 + L/D)$ representation is quite good up to L/D of unity since, within this range, it never deviates more than 3% from the true value of the Clausing factor. The success of Sreekanth's modified equation lies in the fact that most transition and near free-molecule experimental mass flow data tend to an apparent asymptote which is 3% to 6% higher than the free-molecule limit of unity, and his modification "adjusts" the "theoretical" free-molecule limit to 4/3 times 3B/2 ($\sim$1.047).

It is worthwhile to note that the leading term in equation (2-23) for any of the B's of equations (2-20abc) is less than unity; thus equation (2-23) does not even have the proper free-molecule limit of unity. Considering the lack of rigor in the slip flow correction, however, one might be tempted to set this leading term equal to unity. Thus one has

$$\frac{\dot{m}}{\dot{m}_{fm}} \doteq 1 + \frac{3\sqrt{2\pi}}{256} \left(\frac{Ma}{Re}\right)^{-1} \quad . \tag{2-25}$$

Of course, this equation is no more valid than the one attributed to Sreekanth, but it now has the same form as the valid solutions of the near free-molecule flow regime which helps to explain the fascination which some investigators have for this equation. [Compare equation (2-25) to equations (2-8), (2-9), and (2-12).]

III. APPARATUS AND TECHNIQUES

General Description

The apparatus used in this study of rarefied gas flow is a continuous-flow, open-circuit facility which was designed and built by Henderson (14) and McGill (15) to operate over a stagnation chamber pressure range of 1×10^{-6} to 5×10^{-1} atmospheres while maintaining a minimum 100:1 pressure ratio across a test aperture of characteristic dimension 1×10^{-1} centimeters.

Figure 1 is a photograph of the apparatus whose three main component groups are shown schematically in Figures 2, 3, and 4. A list of the equipment comprising the apparatus is given in Table I. Since the schematics are largely self-explanatory, the following paragraphs are devoted to the less obvious details and techniques.

Gas Feed and Flow Measurement

All experiments were performed with CIT grade helium taken from standard cylinders. No particle filters were used, but condensable gases were removed by the use of a liquid nitrogen cold trap. The constant temperature bath was adjusted to maintain a nominal gas output temperature equal to that of the almost-constant temperature of the air-conditioned laboratory.

Two different types of volumetric flow meters were used depending upon the flow rate. For flow rates less than 1 or 2 cc/sec, the vol-u-meter® was used. For flow rates greater than 1 or 2 cc/sec,

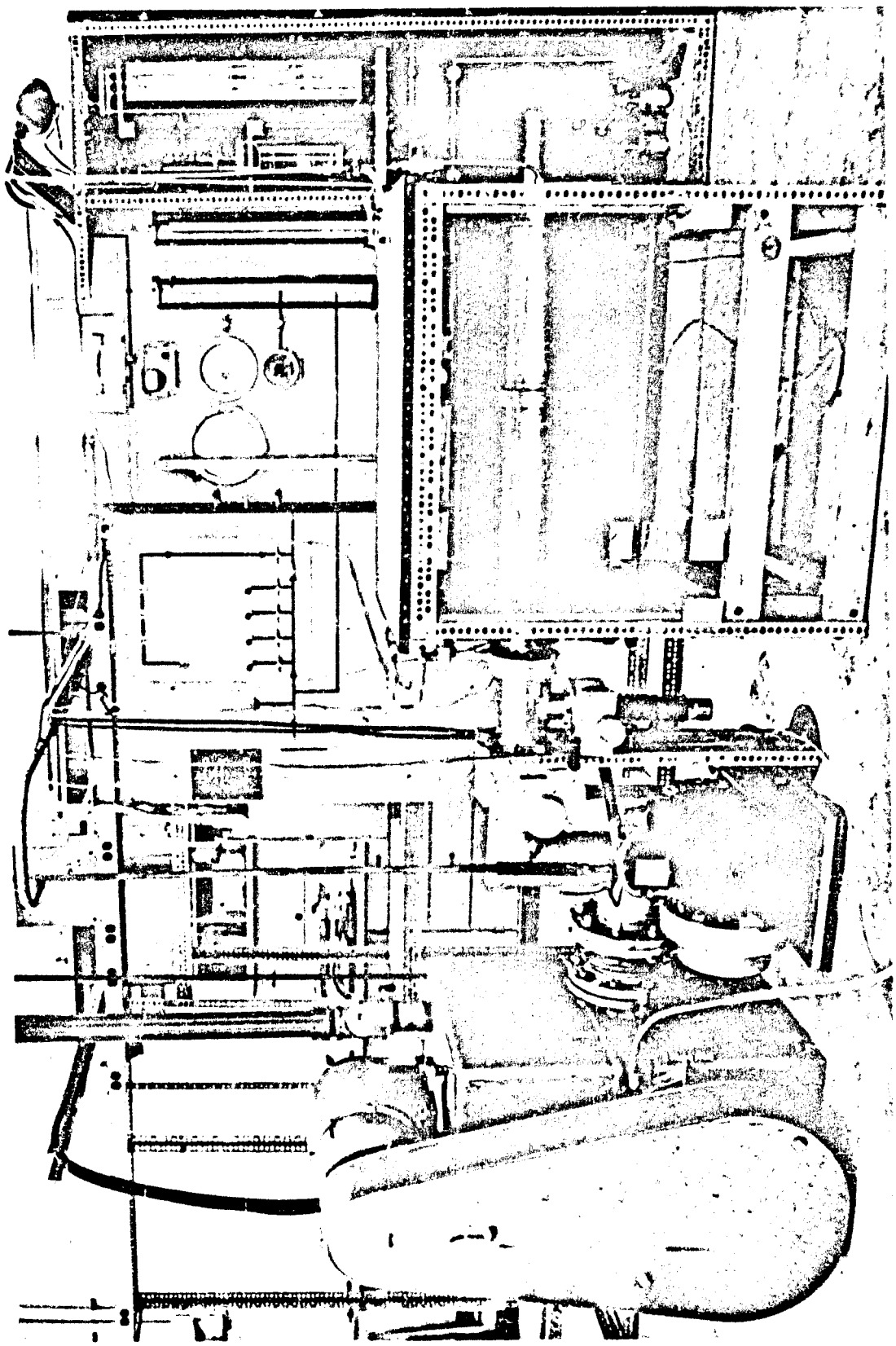

Figure 1. Photograph of apparatus

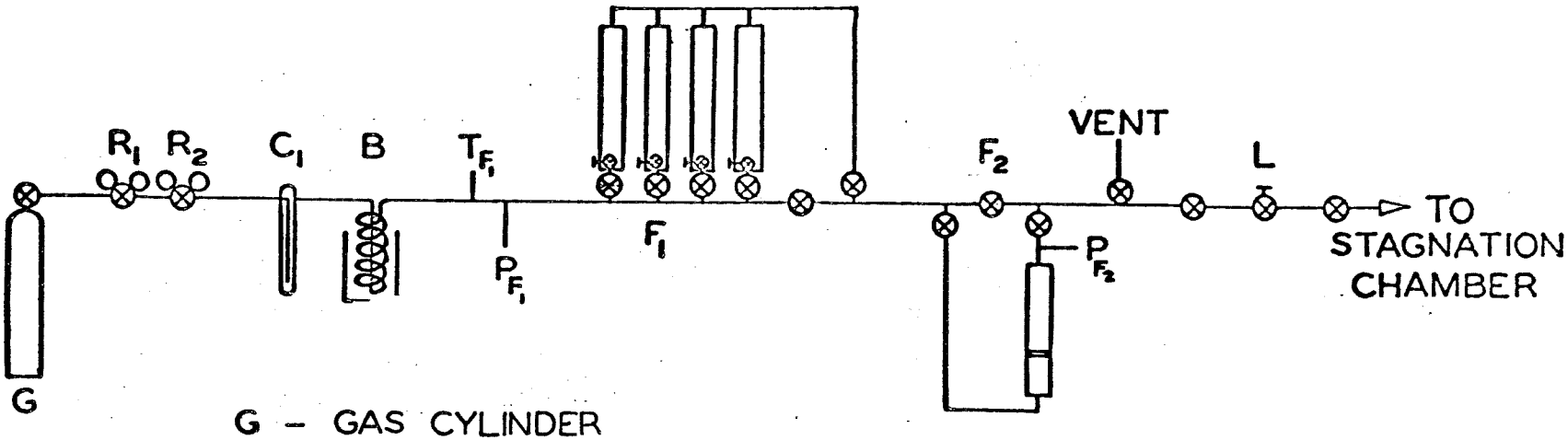

G – GAS CYLINDER
R_1 – HIGH PRESSURE REGULATOR
R_2 – LOW PRESSURE REGULATOR
C_1 – LIQUID NITROGEN TRAP
B – CONSTANT TEMPERATURE BATH
T_{F_1} – TEMPERATURE WELL
P_{F_1} – PRESSURE TAP
F_1 – ROTAMETERS
F_2 – VOL-U-METER
P_{F_2} – PRESSURE TAP
L – VARIABLE LEAK

Figure 2. Gas feed and flow measurement schematic

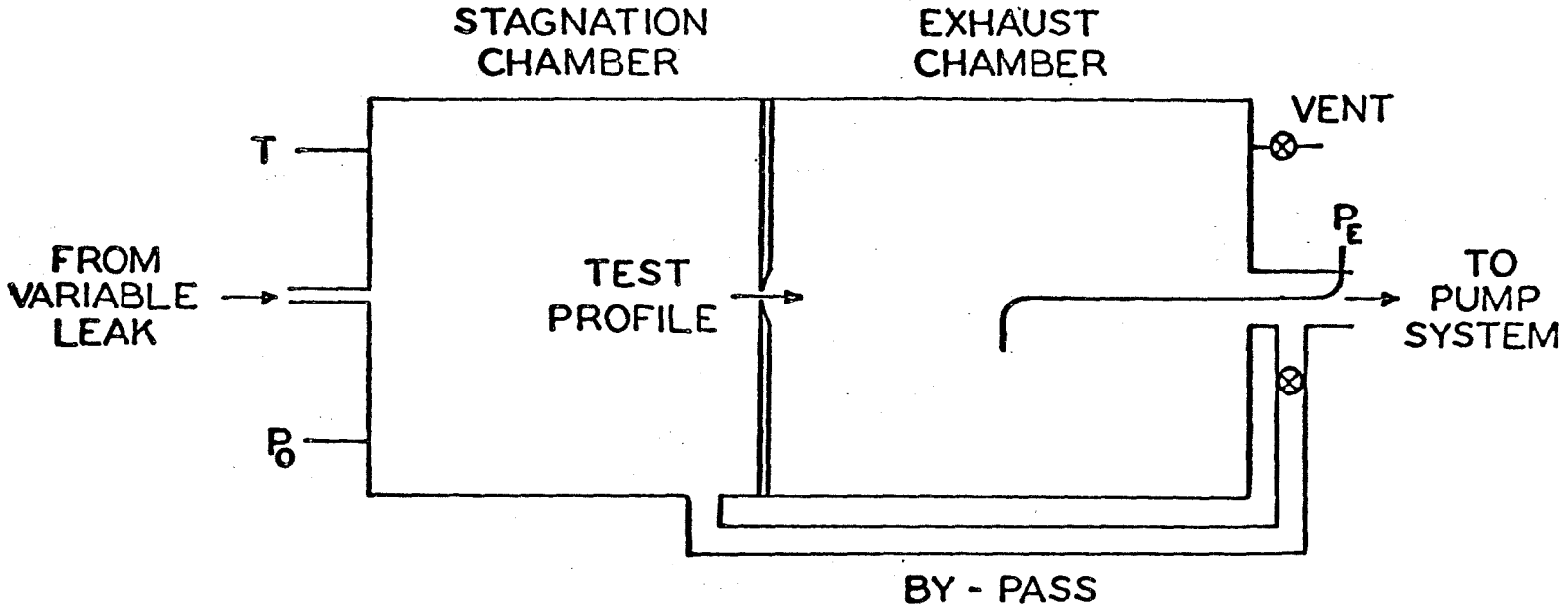

T - TEMPERATURE WELL

P_O - STAGNATION CHAMBER PRESSURE TAP

P_E - EXHAUST CHAMBER PRESSURE TAP

Figure 3. Vacuum test vessel schematic

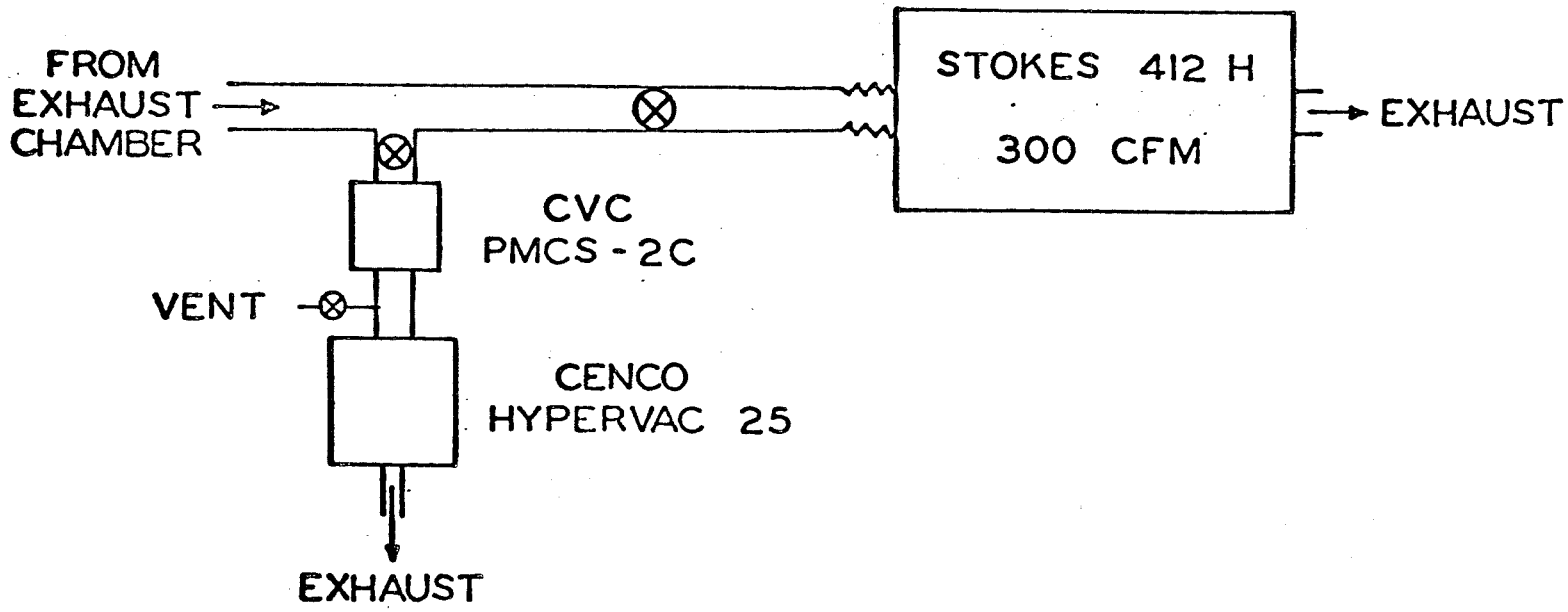

Figure 4. Pumping schematic

TABLE I

LIST OF EQUIPMENT

Item	Description
gas cylinders	2000 psig cylinder of research grade helium of purity $\geq$ 99.99%
	2000 psig cylinder of nitrogen
pressure regulators	Matheson model 1L delivery pressure 3 to 80 psig
	Matheson model 2 delivery pressure 25 to 650 psig
	Matheson model 70B delivery pressure 3 to 15" H_2O gage
liquid nitrogen cold traps	Greiner Glassware double-tube trap 30 cm long
constant temperature bath	ten-gallon jar of water with thermostatically controlled resistance heater
vacuum flasks	Thermos model 8640
thermometers	ASTM Saybolt viscosity #17F range 66 to 80°F least count 2 F°
	Central Scientific range -10 to +120°F least count 2 F°
barometer	Central Scientific
vol-u-meter®	Brooks range 0 to 25 cc accuracy .2% of indicated volume
pumps	Stokes model 412H CENCO hypervac 25 CVC PMCS-2C

TABLE I (continued)

Item	Description
dial gages	Burton model 2311-001 range 0 to 15 psia least count .1 psi
	Wallace and Tiernan model FA-233111 dual range 0 to 25, 25 to 50 psia least count .05 psi
	Wallace and Tiernan model FAR 160 range 0 to 50 mm Hg least count .2 mm Hg
manometers	Wallace and Tiernan model FA 135 range 0 to 800 mm Hg
rotameters	Brooks E/C meters models R-2-15AA with stainless steel float, R-2-25D with sapphire float, R-2-25A with sapphire float, and R-2-25B with sapphire float least count .1 mm
timer	Standard range 0 to 1000 sec least count .1 sec
variable leak	Granville-Phillips model 203 range 10^{-10} cc/sec to 10^{2} cc/sec with 1 atm pressure differential
thermistor gage	CVC model GTC-100 range 0-1000 Hg
McLeod gages	Greiner Glassware non-linear model range 0 to 125μHg
	linear model ranges 0 to 1 mm Hg, 0 to 10 mm Hg, and 0 to 100 mm Hg

one of four rotameters was used. The rotameters, which are continuous-flow devices, were calibrated for helium using the water displacement method. When measuring low flow rates, the vol-u-meter®--a positive displacement device--was bypassed until steady state conditions were attained. At this time it was switched into the circuit to measure the volumetric flow rate. Since this increased the pressure drop across the flow meters, the steady state conditions previously attained were disturbed. A technique whereby one of the rotameter needle valves was used to increase the pressure drop across the flow meters when the vol-u-meter® was bypassed, and was switched out of the circuit when the vol-u-meter® was switched in, appeared to correct this disturbance.

The precision stainless steel needle valve, used to throttle the gas into the stagnation chamber of the vacuum vessel, had a three digit counter attached to the drive handle. Each digit in the unit's position of the counter corresponded to 1/10 turn of the needle valve which required 27 full turns to go from fully open to fully closed conductance. This counter was used as an aid in repeating an experimental point.

Vacuum Test Vessel

The vacuum test vessel is a steel cylinder with end plates and a bulkhead which divides the tank into two chambers. Each chamber measures 40 cm on the internal diameter. The upstream chamber is 40 cm long; the downstream chamber is 50 cm long. The bulkhead has a machined

opening which can accommodate various size test apertures. The apertures are installed or inspected through a port in the upstream stagnation chamber. Three penetrations are provided in the stagnation chamber and two are provided in the exhaust chamber for gas inlet, gas exit, temperature taps, and pressure taps. Considerable care was taken in the selection of these locations so as not to bias the data.

Test Apertures

The circular orifice used in this study was machined from steel plate, inspected on an optical comparator, and fitted flush into the upstream surface of the dividing bulkhead of the vacuum test vessel. Considering the fact that the diameter of the orifice is 1×10^{-1} cm and the internal diameter of the vacuum test vessel is 40 cm, the tank walls do not have any effect on the flow. Figure 5 is a detail drawing of the circular orifice which was used in the present study. The Clausing factor for this geometry is 0.918, and it was obtained from Clausing's (10) original work using the dimensions given in Figure 5.

Several slits were chemically milled in 0.002-inch thick beryllium-copper and inspected on an optical comparator. The slit chosen for use was approximately rectangular when observed under 20 X magnification. Because of the method of construction, the slit had no sharp corners. Based on the actual flow area, it effectively measured 0.0038 inches by 0.35 inches. The flow area of the slit increased very slightly from one side to the other (the slit was acid etched from one side only), so it was used with the flow area increasing in the

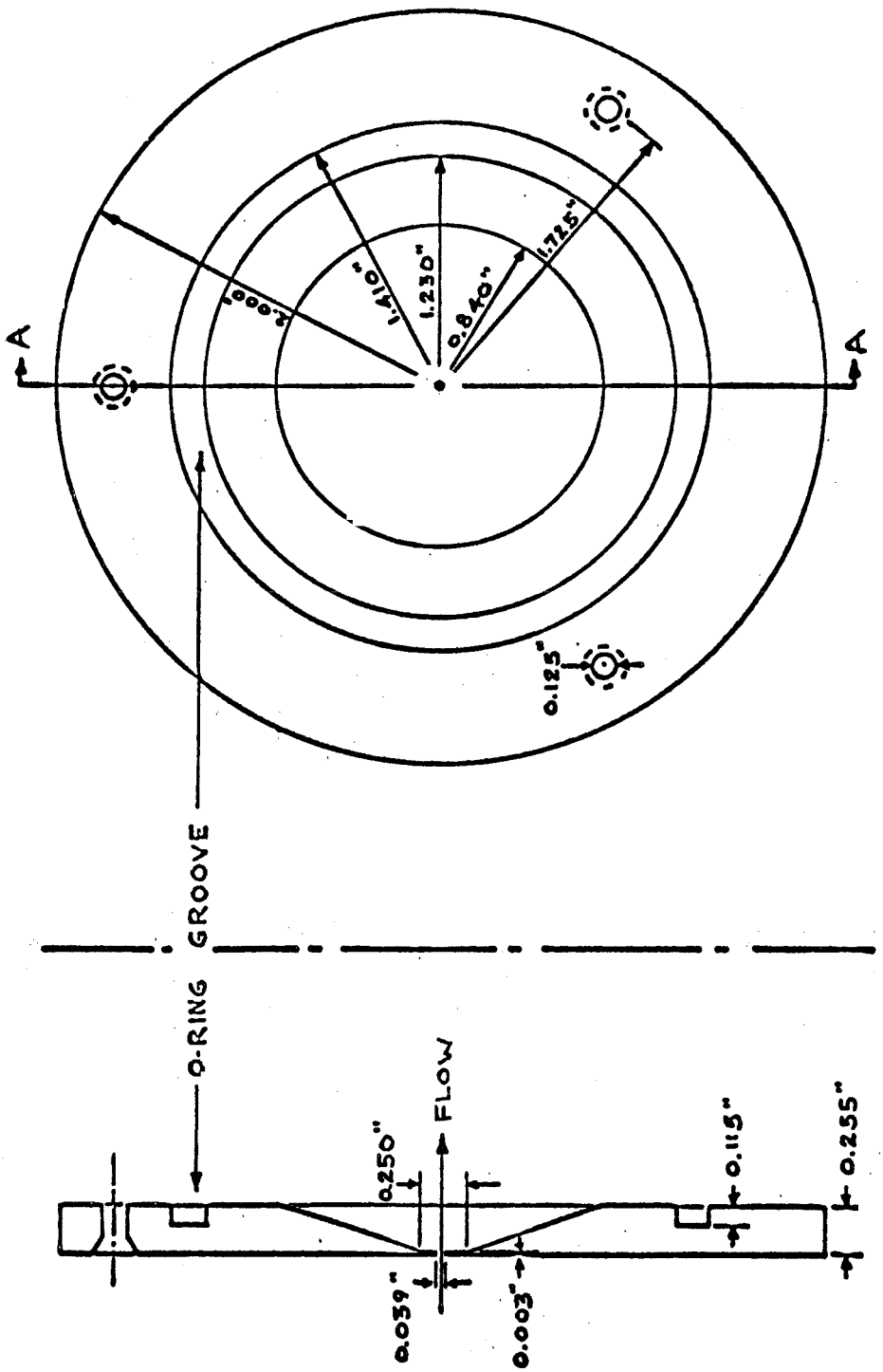

Figure 5. Detail drawing of circular orifice

direction of the flow. The Clausing factor for the slit is 0.6, and it was calculated, assuming rectangular geometry, from formulas in Clausing's (10) original work using the effective dimensions. Even after making allowance for the divergence of the flow area, there is still a greater uncertainty in the slit Clausing factor than in the orifice Clausing factor. Figure 6 shows the effective dimensions of the slit which was used in the present study, the adapter plate, and the manner in which the slit was mounted.

Pumping

The parallel pumping arrangement allows a rapid evacuation of the vacuum test vessel to the 1×10^{-6} atmosphere range by use of the large mechanical pump. During this time, the oil diffusion pump is isolated while being warmed to operating conditions. There is no provision for controlling the backstreaming of the pump oils.

Vacuum Pressure Measurement

Stagnation chamber pressures can be measured by either of two McLeod gages, a mechanical gage, a mercury manometer, or a thermistor gage, depending upon the pressure range. The McLeod gages are the primary standards, and the other instruments are calibrated to agree with them; however, the thermistor gage is only used for pressure monitoring. The exhaust chamber pressure can be measured by either of the same two McLeod gages or a thermistor gage. As before, the thermistor gage is used only for monitoring pressure. All pressure

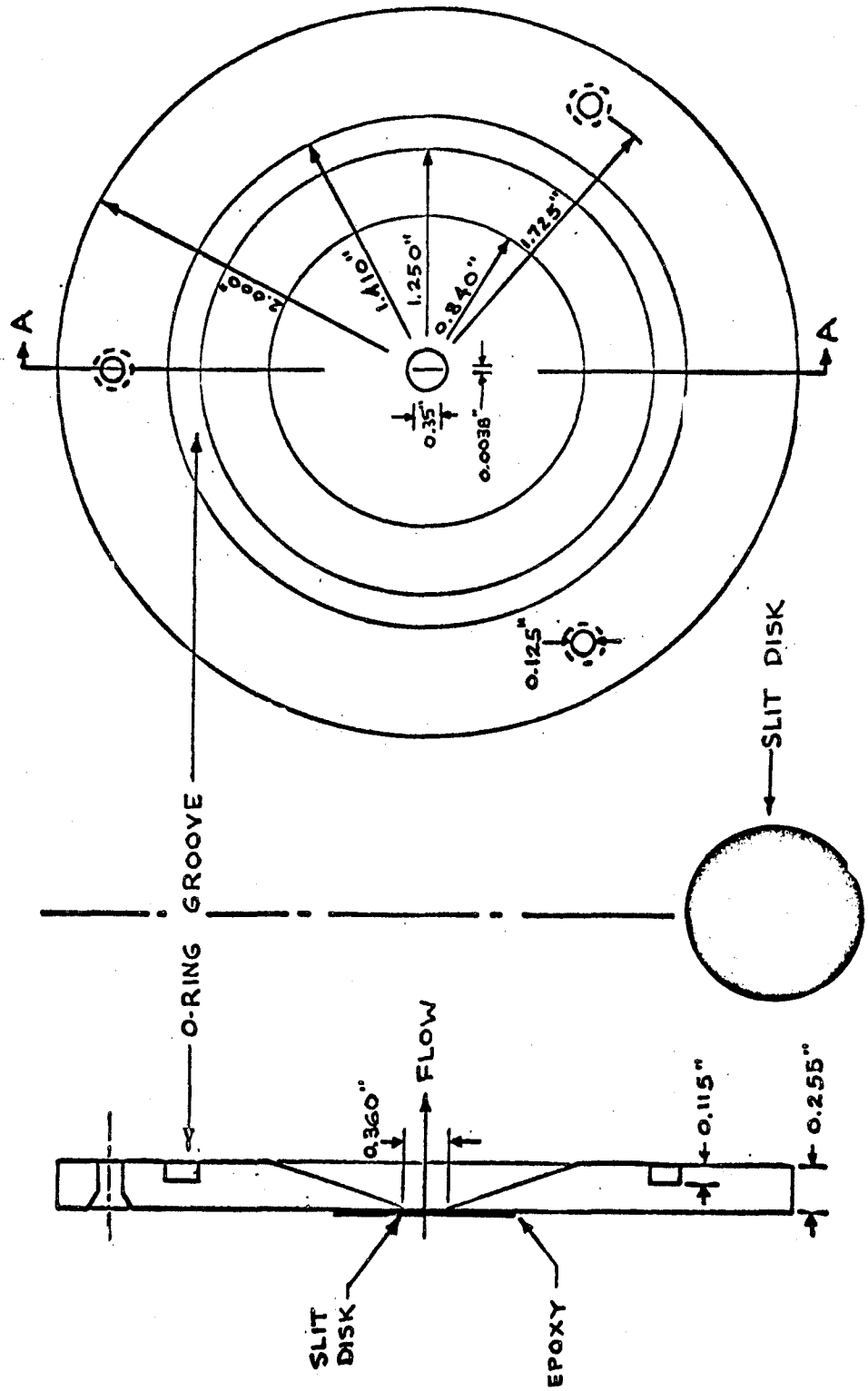

Figure 6. Detail drawing of two-dimensional slit

measurements involving mercury columns were corrected to 0°C and standard gravity.

Seals, Leaks and Outgassing

Extensive use was made of O-ring and glassblown seals in the construction of the apparatus. Where such seals were not used, the joints were coated with epoxy or painted with glyptal®. After the installation or inspection of the test apertures, the vacuum test vessel was pumped to the micron range and held there for several weeks in order to reduce the effects of outgassing. The ultimate leak plus outgassing thus obtained would raise the tank pressure from 10^{-4} mm Hg by approximately .3μ/hr. For all but the smallest flow rates, this pressure rise was entirely negligible.

Accuracy

Each of the plotted points is an average of three or more measurements at the same setting of the precision needle valve and represents a separate measurement of the volumetric flow. The estimated error from known sources, such as the volumetric flow measurements, room temperature variation, and aperture geometry, is about ± 2% for the orifice and about ± 5% for the slit. Additional errors, which are difficult to estimate, arise from such things as uneven outgassing, lack of attainment of steady flow, and the inherent difficulties involved in using and reading a McLeod gage.

IV. DISCUSSION OF RESULTS

The method of data reduction selected for use is similar to that introduced by Liepmann (1). A characteristic velocity, Mach number, and Reynolds number are defined as

$$W = \sqrt{\frac{P_1 - P_2}{\rho_1}} \quad , \tag{4-1}$$

$$Ma = \frac{W}{\sqrt{\frac{P_1}{\rho_1}}} \quad , \tag{4-2}$$

and

$$Re = \frac{WD}{\nu_1} \quad . \tag{4-3}$$

Using the ideal gas equation of state, equation (2-6), these terms can also be written as

$$W = \sqrt{(1 - \frac{P_2}{P_1}) RT_1} \quad , \tag{4-4}$$

$$Ma = \sqrt{1 - \frac{P_2}{P_1}} \quad , \tag{4-5}$$

and

$$Re = \frac{P_1 D \sqrt{1 - \frac{P_2}{P_1}}}{\mu_1 \sqrt{RT_1}} \quad . \tag{4-6}$$

For the large pressure ratios used in this experiment, and in the experiments and theory to which it is compared, these terms are approximately

$$W = \sqrt{RT_1} \quad , \tag{4-7}$$

$$Ma = 1 \quad , \tag{4-8}$$

and

$$Re = \frac{P_1 D}{\mu_1 \sqrt{RT_1}} \quad . \tag{4-9}$$

The characteristic dimension of the circular orifice and of the two-dimensional slit is based on the ratio of aperture area to aperture perimeter. Thus, one has for the circular orifice,

$$D^* = 4\left[\frac{\frac{\pi D^2}{4}}{\pi D}\right] = D \quad , \tag{4-10}$$

and for the slit,

$$D^* = 4\left[\frac{hb}{2(h+b)}\right] = \frac{2b}{1+\frac{b}{h}}$$

$$\left[\longrightarrow \quad 2b \text{ for } \frac{b}{h} << 1\right] \quad , \tag{4-11}$$

where $\frac{b}{h}$ is the ratio of the short side of the slit to the long side of the slit. In these experiments, $\frac{b}{h} << 1$. Note that the ratio of Mach number to Reynolds number,

$$\frac{Ma}{Re} = \frac{\sqrt{1 - \frac{p_2}{p_1}}}{\frac{p_1 D \sqrt{1 - \frac{p_2}{p_1}}}{\mu_1 \sqrt{RT_1}}} = \frac{\mu_1 \sqrt{RT_1}}{p_1 D} \quad , \tag{4-12}$$

is proportional to the Knudsen number,

$$Kn = \frac{\lambda}{D^*} \quad ; \tag{4-13}$$

but it avoids the ambiguity associated with the definition of a mean free path.

As $\frac{Ma}{Re} \longrightarrow \infty$, the theoretical limit for each geometry is

$$\lim_{\frac{Ma}{Re} \to \infty} \frac{\dot{m}}{\dot{m}_{fm}} = 1 \quad . \tag{4-14}$$

As $\frac{Ma}{Re} \longrightarrow 0$, the theoretical limit for each geometry is given by

$$\lim_{\frac{Ma}{Re} \to 0} \frac{\dot{m}}{\dot{m}_{fm}} = \frac{a}{\kappa} \left[2\pi\gamma \left(\frac{2}{\gamma + 1} \right)^{\frac{\gamma + 1}{\gamma - 1}} \right]^{\frac{1}{2}} \left[1 - \frac{p_2}{p_1} \right]^{-1} \quad . \tag{4-15}$$

Note that this limit, as defined, is a function of the aperture geometry (κ), the pressure ratio $\frac{p_2}{p_1}$, and the molecular complexity of the gas (γ); whereas the free-molecule flow limit, as defined, is independent of such factors and α.

Except for one figure, which is plotted as the ratio of measured mass flow to theoretical continuum limit mass flow versus the ratio of Mach number to Reynolds number, the results of the present investigation and the results of previous investigators are plotted as the ratio of measured mass flow to theoretical free-molecule mass flow versus the ratio of Mach number to Reynolds number.

Figure 7a shows the present experimental data for the circular orifice and the two-dimensional slit. Note how the dimensionless mass flow for each aperture levels off near $\frac{Ma}{Re} = 10^{o}$ as the free-molecule flow limit is approached. Since the data levels off well above the theoretical limit of unity, there is probably some systematic error here which involves the flow area, the Clausing factor, and the pressure difference across the apertures; yet, it is interesting to note that the original data of Knudsen (13), when corrected for finite aperture thickness by Liepmann (1), are about 7% greater than the limiting value in this region. In addition, although Sreekanth (3) used very precise instrumentation and a circular orifice 1 inch in diameter in 0.005-inch thick copper, even his data are 4% greater than the limiting value in this region. According to the theoretical calculations on nearly free-molecule flow, however, the mass flow ratio should be within 2% of its limiting value in this region. There is no very satisfactory explanation

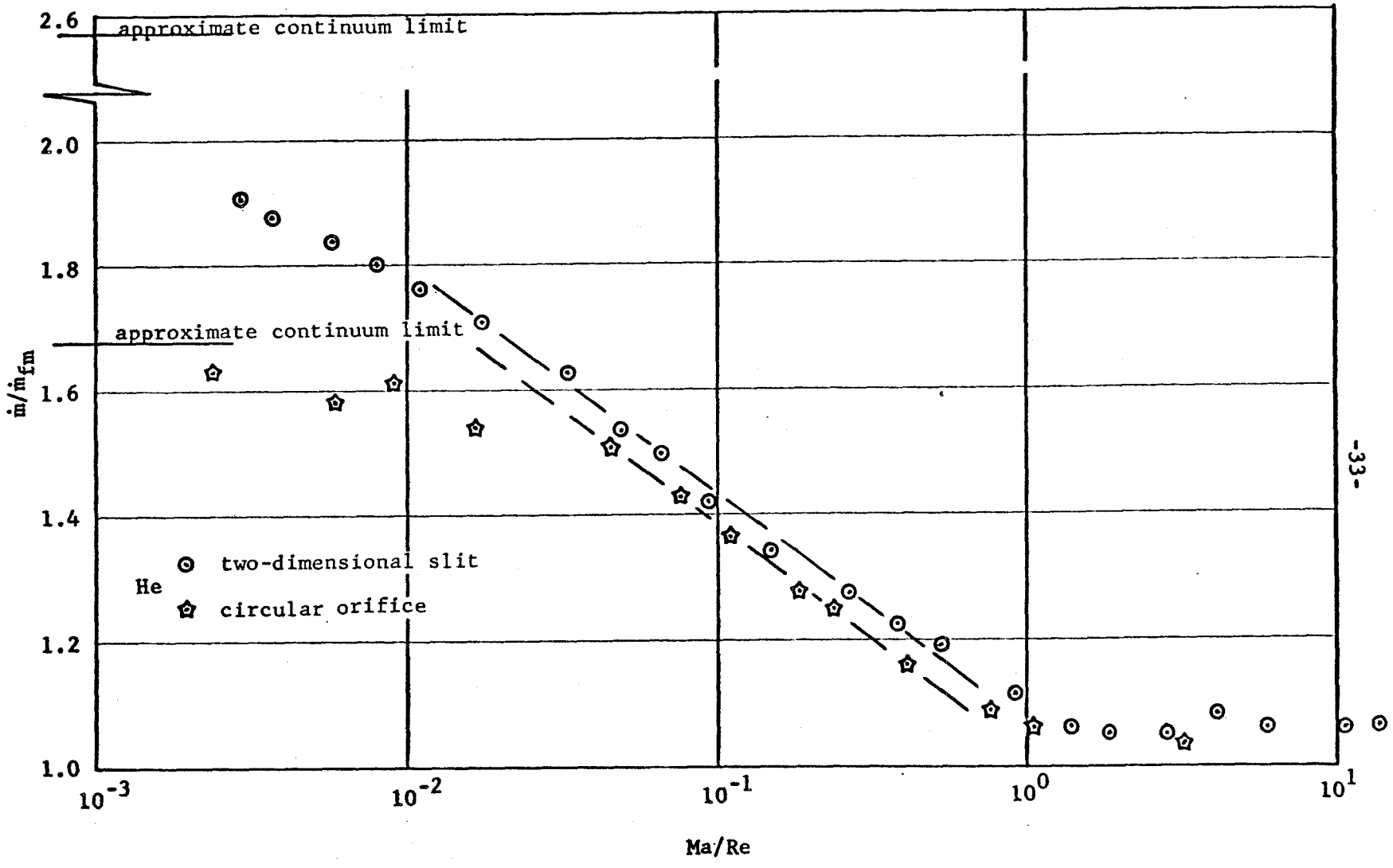

Figure 7a. Plot of experimental data for circular orifice and two-dimensional slit

for this behavior other than the factors mentioned above. For values of $\frac{Ma}{Re} < 5 \times 10^{-2}$, the data for the orifice and the slit diverge greatly. One should expect this behavior because of the large difference in the continuum limits of the two apertures, a result of the greatly different Clausing factors for the two apertures and the manner in which the continuum limit is defined in equation (4-15). Since the Clausing factor for the orifice used in the present investigation is 0.918, and that for the slit is 0.6, other things being equal, one can see from equation (4-15) that the defined continuum limit for the slit is 0.918/0.6 times that of the orifice.

Excluding the uncertainty in the difference between α for the circular orifice and α for the two-dimensional slit, one might attempt to infer that the difference in the dimensionless mass flow for an orifice and a slit which have identical Clausing factors could be quite small over the whole flow spectrum. That this inference is invalid is easily seen when one examines Figure 7b where the experimental mass flow of the present investigation is made dimensionless, using the theoretical continuum-limit mass flow. This figure vividly illustrates the fact that there is quite a difference in the flow through a circular orifice and a two-dimensional slit. Probably the most striking difference to be noted in Figure 7b is in the approach to the continuum limit. For values of $\frac{Ma}{Re}$ of order 10^{-3} the orifice mass flow is within a few percent of the continuum limit while the slit mass flow is very far away from the continuum limit. A crude estimate, obtained by linear extrapolation in Figure 7b, indicates that the slit flow will require values of $\frac{Ma}{Re}$ of

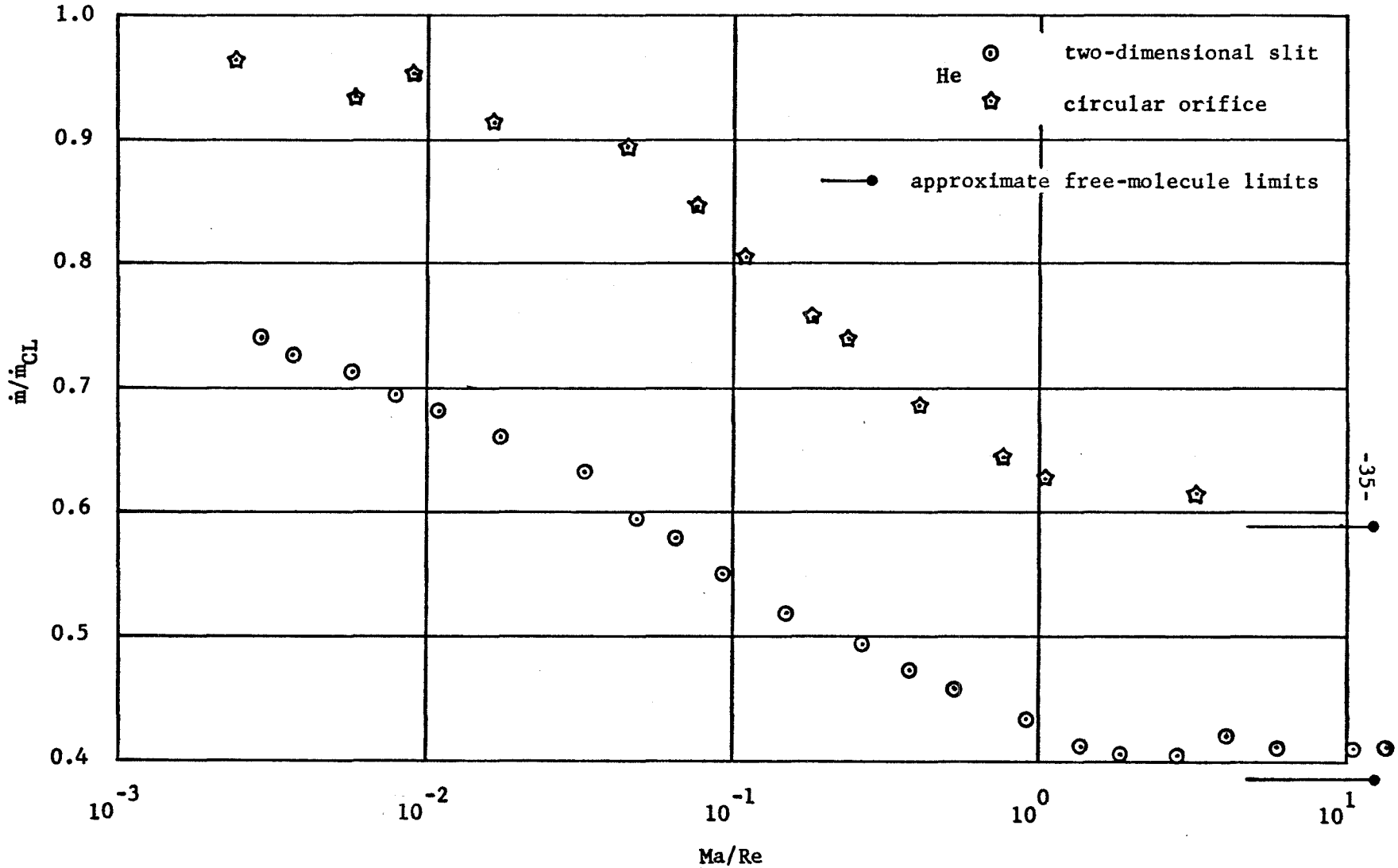

Figure 7b. Plot of experimental data for circular orifice and two-dimensional slit (modified)

order 10^{-4} in order to approach the continuum limit as closely as the orifice flow does at values of $\frac{Ma}{Re}$ of order 10^{-2}.

Figure 8 compares the data of the present investigation with the experimental data of Liepmann (1), Henderson (14), and McGill (15) for orifice flow. The agreement is seen to be quite good in all respects for $\frac{Ma}{Re} > 5 \times 10^{-2}$. As previously mentioned, the divergence at the continuum end of the flow spectrum is due to the different Clausing factors. The Clausing factor for Liepmann's orifice is 0.975 which places its continuum limit lower than that for the circular orifice used by Henderson, McGill, and the present investigator.

Figure 9 compares the data of the present investigation with the theoretical calculations of Narasimha (4) and Willis (2) for the region near free-molecule flow $\left(\frac{Ma}{Re} \geq 1\right)$. In this limited range, the agreement is qualitatively good but quantatively poor, for the experimental data levels off too high. One must remember that the calculations of Narasimha and Willis are only valid for $\frac{Ma}{Re} \geq 1$; therefore, they cannot be legitimately compared to the experimental data outside this range.

Figure 10 compares the data of the present investigation with the experimental data of Sreekanth (3) for orifice flow. Within the limited range of Sreekanth's data, the agreement of his orifice flow and that of the present investigator is quantitatively good and qualitatively excellent.

Figure 11 compares the data of the present investigation with the experimental data of Smetana (6) and Lord (8) for orifice flow.

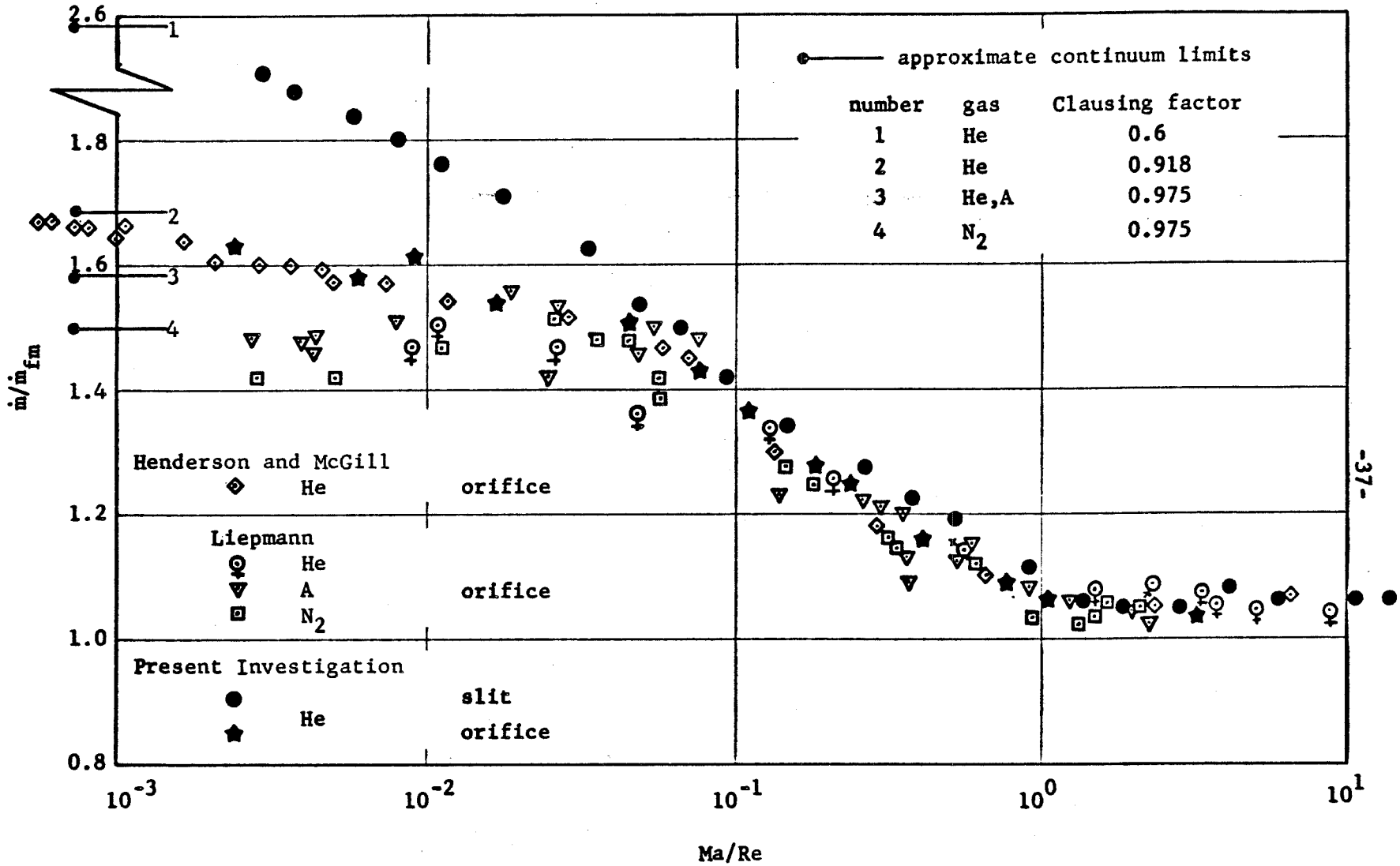

Figure 8. Comparison of present data to that of Liepmann, Henderson, and McGill

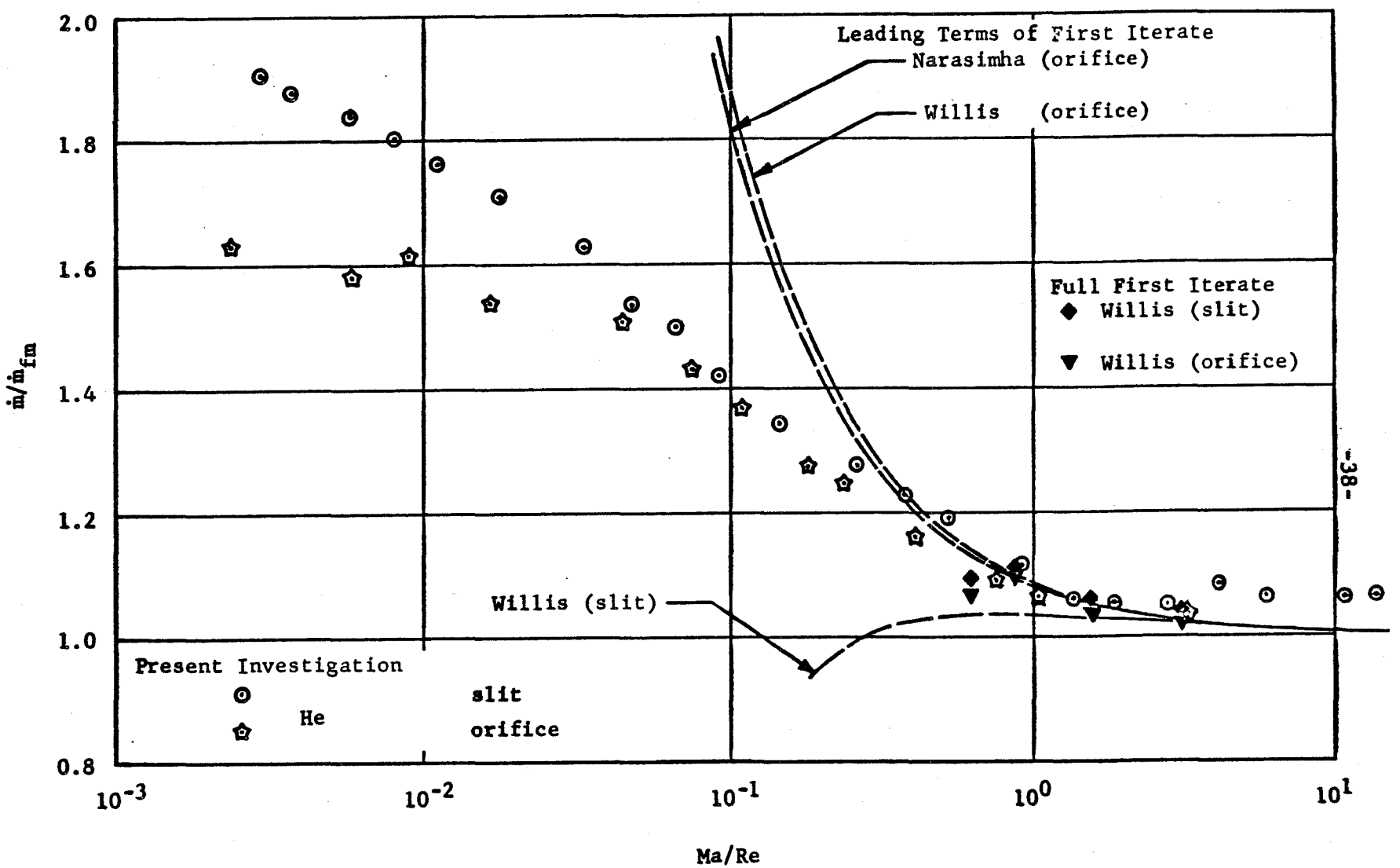

Figure 9. Comparison of present data to that of Narasimha and Willis

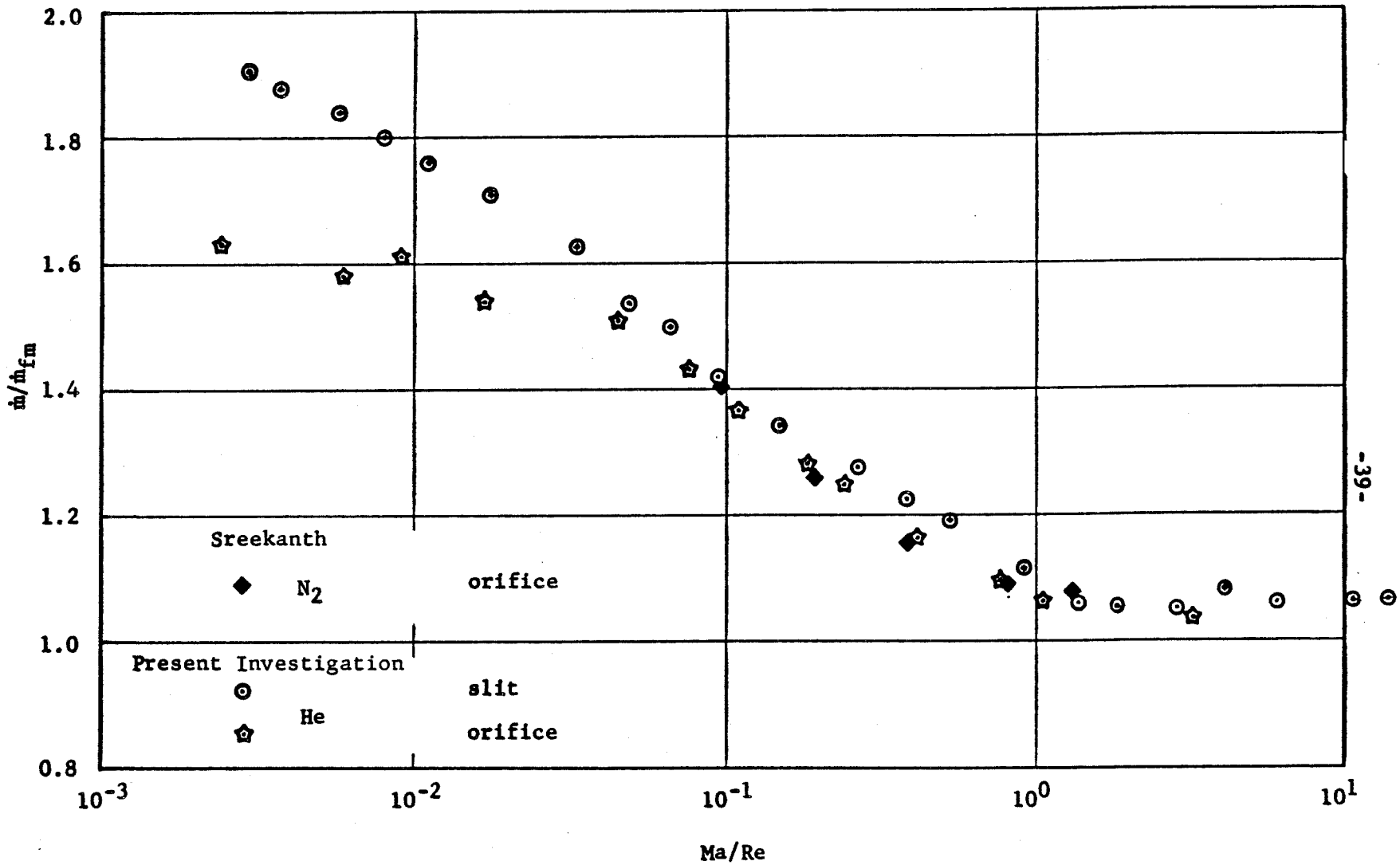

Figure 10. Comparison of present data to that of Sreekanth

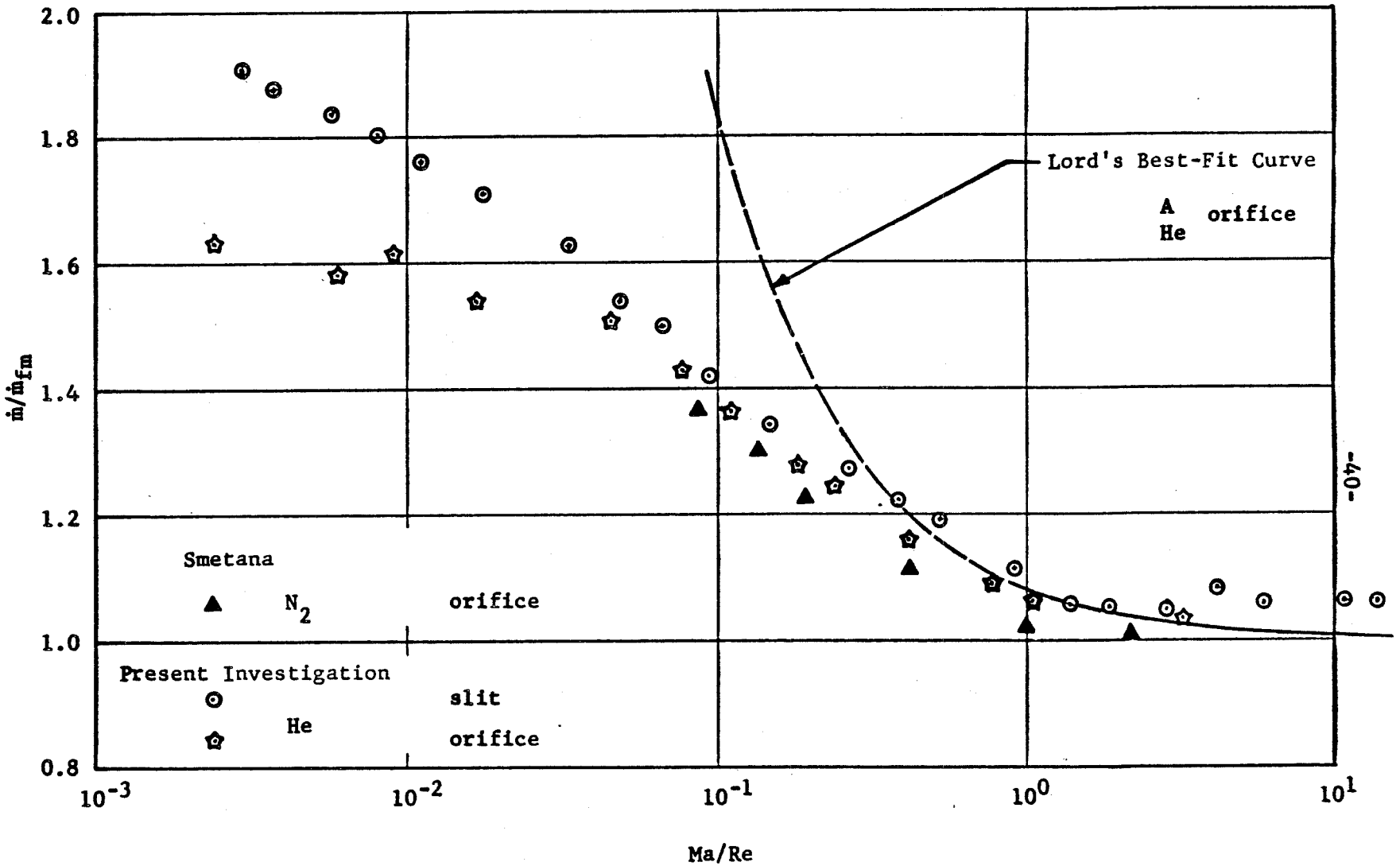

Figure 11. Comparison of present data to that of Smetana and Lord

Smetana's experimental data are shown, while Lord's data are represented by his best-fit curve. The agreement of the three sets of orifice data is fairly poor. It should be noted, however, that Lord's experimental range is $\frac{Ma}{Re} \geq 1$. Therefore, his data should not be compared to other data outside this range. Smetana's data do not appear to be corrected for nonzero orifice thickness. If corrected for this effect, his experimental points would be increased about 1%.

Figure 12 compares the data of the present investigation with various forms of the modified Poiseuille equation [equation (2-22)]. This figure is included here strictly as a matter of interest and information, and one is directed to the section on Slip and Transition Flow (pages 11-15) for all comments.

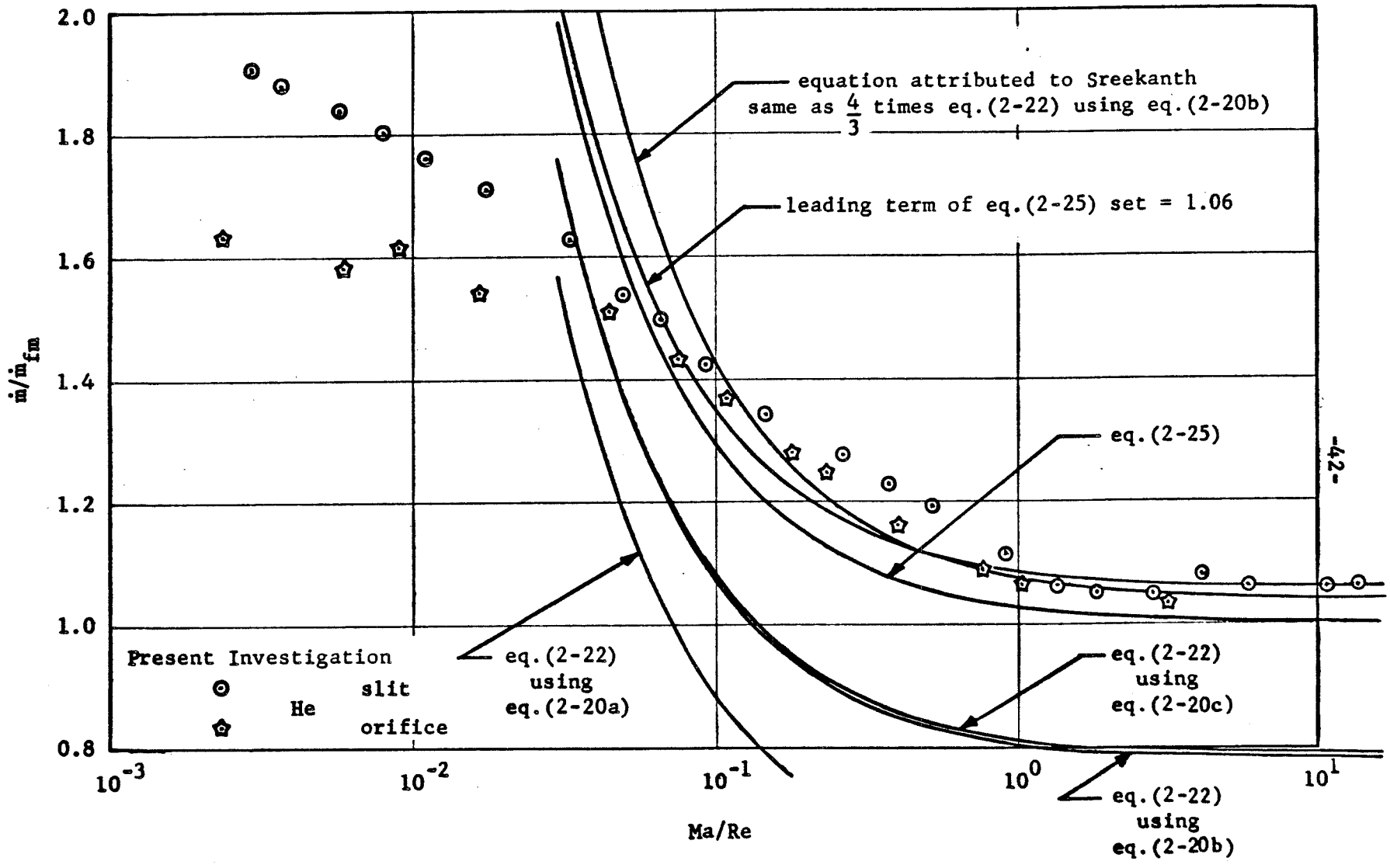

Figure 12. Comparison of present data to the modified Poiseuille equations

V. CONCLUSIONS

The experiments conducted on the circular orifice and the two-dimensional slit show the trend of asymptotic approach to a limiting value at each end of the flow spectrum, corresponding to the continuum flow limit and the free-molecule flow limit. The transition from one part of the flow spectrum to another is smooth, as attested to by the smooth curves of dimensionless mass flow versus dimensionless rarefaction parameter. The data of the present investigation, and that of all other investigations surveyed except one, show a mass flow, in the nearly free-molecule part of the flow spectrum ($10^{0} \leq \frac{Ma}{Re} \leq 10^{1}$), which is greater than that predicted by the theoretical analysis. As discussed on page 32, this is thought to be experimental error; yet, the disparity lies outside the estimated limits of experimental error of each investigation. Future investigations will be necessary to resolve this question.

One of the most surprising aspects of the present investigation is the fact that the transition from near free-molecule flow to near continuum-limit flow for the two-dimensional slit appears to cover a much broader range of the flow spectrum than that required for the circular orifice. The transition for the circular orifice appears to be substantially complete within the range $10^{-2} \leq \frac{Ma}{Re} \leq 10^{0}$ (see Figure 7b). The transition for the two-dimensional slit is roughly estimated to cover the range $\sim 10^{-4} \leq \frac{Ma}{Re} \leq 10^{0}$ (see Figure 7b and the discussion on page 34).

It is interesting to note how the leading term of equations similar to equation (2-23) can be adjusted to give good agreement with

the flow in the range $Ma/Re \geq 10^{-1}$. The obvious reason for the success lies, of course, in the fact that the first iterate of the rigorous gaskinetic solution for this range is linear in $(Ma/Re)^{-1}$ as is equation (2-23).

In conclusion, the flow of a rarefied gas through a thin aperture of arbitrary geometry is worthy of further investigation. Theoretically, one needs to determine a general formula for the $\alpha(\gamma)$ factor and to analyze the flow near the continuum limit. Experimentally, one needs to get the apparent free-molecule limit to agree (at least within the experimental error) with the theoretical free-molecule limit.

BIBLIOGRAPHY

BIBLIOGRAPHY

1. Liepmann, H. W. "Gaskinetics and Gasdynamics of Orifice Flow," Journal of Fluid Mechanics, Vol. 10, Part I (1961), 65-79.

2. Willis, D. R. "Mass Flow Through a Circular Orifice and a Two-Dimensional Slit at High Knudsen Numbers," Journal of Fluid Mechanics, Vol. 21, Part I (1965), 21-31.

3. Sreekanth, A. K. "An Experimental Investigation of Mass Flow Through Short Circular Tubes in the Transition Flow Regime," Boeing Document D1-82-0427, Boeing Scientific Research Laboratories (1965).

4. Narasimha, Roddam. "Orifice Flow at High Knudsen Numbers," Journal of Fluid Mechanics, Vol. 10, Part 3 (1961), 371-384.

5. Milligan, M. W. "Low-Density Gas Flow in Long Tubes," AIAA Journal, Vol. 4, No. 4 (1966), 745-746.

6. Smetana, F. O. "Measurements of the Discharge Characteristics of Sharp-Edged and Round-Edged Orifices in the Transition Regime," Rarefied Gas Dynamics, Vol. II (1967), 1243-1256.

7. Carley, C. T., Jr. "Experiments on Transition Regime Flow Through a Short Tube with a Bellmouth Entry," AIAA Journal, Vol. 4, No. 1 (1966), 47-54.

8. Lord, R. G. "Nearly Free Molecule Flow Through a Circular Orifice at High Pressure Ratios," Rarefied Gas Dynamics, Vol. II (1967), 1235-1242.

9. Present, R. D. Kinetic Theory of Gases. New York: McGraw-Hill, 1958.

10. Clausing, P. "Über die Strömung sehr verdunnter Gase durch Rohren von beliebiger Lange," Ann. Physik, Vol. 12 (1932), 961-989.

11. Guderley, K. G. Theorie Schallnaher Strömungen. Berlin: Springer-Springer-Verlag, 1957.

12. Frankl, F. I. "The Discharge of a Supersonic Jet from a Vessel with Plane Walls," Reports of the Academy of Sciences USSR, Vol. 58, No. 3 (1947), 381-384. (In Russian)

13. Knudsen, M. "Die Gesetze der Molekularströmung und der inneren Reibungsstromung der Gase durch Röhren," Ann. Physik, Vol. 28 (1909), 75-130.

14. Henderson, A. H. "Construction and Testing of a Rarefied Gas Flow Facility." Aeronautical Engineer's thesis, California Institute of Technology, Pasadena, 1967.

15. McGill, J. A. "Low-Density Gas Facility." Aeronautical Engineer's thesis, California Institute of Technology, Pasadena, 1967.